Quantum Opt. 4 (1992) 245–263. Printed in the UK

Number and phase quantum fluctuations in the down-conversion with a quantum pump

R Tanaś† and Ts Gantsog‡

Laboratory of Theoretical Physics, Joint Institute for Nuclear Research, Dubna, Head Post Office PO Box 79, Moscow 101000, Russia

Received 3 October 1991, in final form 6 February 1992

Abstract. The photon number and phase quantum fluctuations in the field produced by the down-conversion process with a quantum pump are studied. The fully quantum approach using the method of numerical diagonalization of the interaction Hamiltonian is applied to find the evolution of the system. The evolution of the photon number fluctuations, the joint number of photons probability distribution, the quadrature variances, the joint phase probability distribution, the marginal number and phase distributions for the signal mode, the number and phase uncertainty products and squeezing parameters are calculated and illustrated graphically. The results for the signal mode are compared to the corresponding results for the ideal squeezed vacuum to show the range of validity of the parametric approximation.

1. Introduction

The parametric down-conversion process is a well known non-linear process that produces optical fields with non-classical properties [1–10]. It is essential for the quantum properties of fields generated in the process that the high-frequency pump photons are split into highly correlated pairs of lower-frequency signal and idler photons. In the simplest case of a non-depleted degenerate parametric process, the pump mode is assumed as classical and non-depleted, and the signal and idler modes become one mode of the subharmonic field with half the frequency of the pump mode. In this case the time evolution of the subharmonic field can be found analytically and is described by a Bogoliubov transformation that maps the initial vacuum state into an ideal squeezed state [1–6]. The parametric down-conversion process turned out in practice to be very effective in producing squeezed states [11–16].

The states produced by the two-photon down-converter have interesting phase properties studied recently by Vaccaro and Pegg [17], Schleich *et al* [18] and Grønbech-Jensen *et al* [19] for the process with a classical pump and by Gantsog *et al* [20] for the process with a quantum pump. The phase distribution of such states has two sharp peaks at the initial stages of the evolution that reflect the two-photon character of the process. If the quantum fluctuations of the pump mode are taken into

† Permanent address: Nonlinear Optics Division, Institute of Physics, Adam Mickiewicz University, 60-780 Poznań, Poland.

‡ Permanent address: Department of Theoretical Physics, Mongolian State University, Ulan Bator 210646, Mongolia.

0954-8998/92/040245 + 19 $4.50

account the two peaks of the signal mode are broadened, and in the long-time limit the phase distribution becomes uniform [20].

The parametric approximation assuming the pump mode as classical and non-depleted, which leads to closed form analytical solutions for the ideal squeezed states, is not applicable if a considerable amount of power is transferred from the pump mode into the signal mode. In such situations the pump mode must be treated dynamically and its quantum mechanical evolution must be taken into account. Since no closed form solutions are known in this case, some approximations or numerical calculations are needed to find the field evolution. Owing to energy conservation the intensity of the signal mode cannot grow infinitely, and the solutions become oscillatory. The field states of the signal mode are no longer ideal squeezed states, and their properties become different.

In this paper we study the photon number and phase quantum fluctuations in the field produced in the down-conversion process with a quantum pump. The fully quantum approach using the method of numerical diagonalization of the interaction Hamiltonian [21] is employed for getting the evolution of the system. The evolution of quantities such as the photon number fluctuations in both signal and pump modes, the joint phase probability distribution, the joint number of photons probability distribution, the quadrature variances, the marginal number and phase distributions for the signal mode, the number and phase variances for both modes, the number and phase uncertainty products and the number and phase squeezing parameters are obtained and illustrated graphically. The results for the signal mode are compared to the corresponding results for the ideal squeezed states to show the range of validity of the parametric approximation. The Hermitian phase formalism of Pegg and Barnett [22–24] is used to describe the phase properties of the field.

2. Quantum evolution of the field state

The two-photon down-conversion process is described by the following model Hamiltonian

$$H = H_0 + H_I = \hbar\omega a^\dagger a + 2\hbar\omega b^\dagger b + \hbar g(b^\dagger a^2 + b a^{\dagger 2}) \tag{1}$$

where $a(a^\dagger)$ and $b(b^\dagger)$ are the annihilation (creation) operators of the signal mode at frequency ω and the pump mode at frequency 2ω, respectively. The coupling constant g in the interaction Hamiltonian H_I, which is assumed real, describes the coupling between the two modes. The Hamiltonian (1) is identical to that for the second-harmonic generation, and these are the initial conditions that distinguish between the two processes. In the case of harmonic generation mode b is initially in the vacuum state and mode a is populated. For the down-conversion process discussed in this paper, mode b (pump mode) is initially populated, while mode a (signal mode) is in the vacuum state. The distinction between the two processes is far from being trivial, and the states generated in the two processes have quite different properties.

Since H_0 and H_I commute, there are two constants of motion, H_0 and H_I. H_0 determines the total energy stored in both modes, which is conserved by the interaction H_I. This allows us to factor out $\exp(-iH_0t/\hbar)$ from the evolution operator and, in fact, to drop it altogether. In effect, the resulting state of the field can be written as

$$|\Psi(t)\rangle = \exp(-i H_I t/\hbar)|\Psi(0)\rangle \tag{2}$$

where $|\Psi(0)\rangle$ is the initial state of the field. If the Fock states are used as basis states, the interaction Hamiltonian H_I is not diagonal in such a basis. To find the state evolution, we apply the numerical method of diagonalization of H_I [21].

Let us assume that initially there are n photons in the pump mode (b) and no photons in the signal mode (a), i.e. the initial state of the field is $|0, n\rangle = |0\rangle_a|n\rangle_b$. Since H_0 is a constant of motion, we have the relation

$$\langle a^\dagger a\rangle + 2\langle b^\dagger b\rangle = \text{constant} = 2n \tag{3}$$

which implies that the annihilation of k photons of the pump mode requires creation of $2k$ photons of the signal mode. Thus, for given n, we can introduce the states

$$|\psi_{n-k}^{(2n)}\rangle = |2k, n-k\rangle \qquad k = 0,1,\ldots,n \tag{4}$$

which form a complete basis of states of the field for given n. We have

$$\langle\psi_{n'-k'}^{(2n')}|\psi_{m-l}^{(2n)}\rangle = \delta_{nn'}\delta_{kk'} \tag{5}$$

which means that the constant of motion H_0 splits the field space into orthogonal subspaces, which for given n have a number of components equal to $n+1$. The basis states $|\psi_{n-k}^{(2n)}\rangle$ given by (4) are numbered by the total energy (in units of $\hbar\omega$) which is $2n$ and by the number of photons in the pump mode which is $n-k$. Such a choice of indices makes it easier to compare the results obtained for the second-harmonic generation [25, 26] and the two-photon down-conversion process considered here. In fact, if we replace $n-k \to k'$ and $2n \to n'$, we get the states $|\psi_{k'}^{(n')}\rangle$ used to describe the second-harmonic generation. This means that in the 'primed' notation the matrix elements of the interaction Hamiltonian are the same as for the second-harmonic generation, and they are given by [26]

$$\begin{aligned}\langle\psi_{k'+1}^{(n')}|H_I|\psi_{k'}^{(n')}\rangle &= \langle\psi_{k'}^{(n')}|H_I|\psi_{k'+1}^{(n')}\rangle \\ &= \hbar g[(k'+1)(n'-2k')(n'-2k'-1)]^{1/2}.\end{aligned} \tag{6}$$

This allows us to use the same computer program that we used in the case of the second harmonic to diagonalize the interaction Hamiltonian. If the matrix U is the unitary matrix that diagonalizes the interaction Hamiltonian matrix given by (6), i.e.

$$U^{-1}H_I^{(n')}U = \hbar g \times \text{diag}(\lambda_0, \lambda_1, \ldots, \lambda_n) \tag{7}$$

we get as a result of the diagonalization procedure the eigenvalues λ_i of the interaction Hamiltonian (in units of $\hbar g$) and the elements of the matrix U which are defined for given n' (to shorten the notation we have omitted the additional index n').

To find the state evolution, we need the matrix elements of the evolution operator

$$c_{2n,k}(t) = \langle\psi_{n-k}^{(2n)}|\exp(-iH_I t/\hbar)|\psi_n^{(2n)}\rangle. \tag{8}$$

Knowing the eigenvalues λ_i and the elements of the unitary matrix U, we can calculate the coefficients $c_{2n,k}(t)$ according to the formula

$$c_{2n,k}(t) = \sum_{i=0}^{n} \exp(-ig\lambda_i)U_{n-k,i}U_{n,i}^*. \tag{9}$$

A comparison of the coefficients (9) with the coefficients that describe the second-harmonic generation [26] shows that the only difference between the two sets consists

in the different matrix elements of the matrix U that define them. In fact, one can introduce generalized coefficients

$$c^{(n')}_{k',k}(t) = \langle \psi^{(n')}_{k'} | \exp(-\mathrm{i}H_1 t/\hbar) | \psi^{(n')}_{k} \rangle$$
$$= \sum_{i=0}^{[n'/2]} \exp(-\mathrm{i}gt\lambda^{(n')}_i) U^{(n')}_{k',i} U^{(n')*}_{k,i} \tag{10}$$

where $[n'/2]$ is the integer part of $n'/2$. These coefficients can be used to describe the field evolution for any initial conditions, the vaccum not necessarily being one of the modes.

Since, for real g, the interaction Hamiltonian matrix has real elements, the transformation matrix U is a real orthogonal matrix, so the asterisk can be omitted in (9) and (10). Moreover, due to the symmetry of the Hamiltonian the eigenvalues λ_i are distributed symmetrically with respect to zero, with one eigenvalue equal to zero if there is an odd number of them. When the eigenvalues are numbered from the lowest to the highest value, there is an additional symmetry relation

$$U^{(n')}_{k',i} U^{(n')}_{ki} = (-1)^{k-k'} U^{(n')}_{k',[n'/2]-i} U(n')_{k,[n'/2]-i} \tag{11}$$

which makes the coefficients $c^{(n')}_{k',k}(t)$ either real ($k-k'$ even) or imaginary ($k-k'$ odd). This property of the coefficients is very important and allows exact analytical results to be obtained.

The assumption that the signal mode at frequency ω is initially in the vaccum state reduces the number of coefficients to those given by equation (9). One immediate consequence of this assumption is that, according to the conservation law (3), only the sectors of the Hilbert space with $n' = 2n$ contribute to the state evolution, i.e. photons of the signal mode are created in pairs. This is not the case if the second-harmonic generation is considered [26], when all sectors with both odd and even n' contribute to the state evolution.

In this paper we assume that initially the signal mode is in the vacuum state, whereas the pump mode is in a coherent state, so the initial state of the field is

$$|\psi(0)\rangle = \sum_{n=1}^{\infty} b_n |0, n\rangle \tag{12}$$

where

$$b_n = \exp(-|\beta|^2/2)\beta^n/\sqrt{n!} \tag{13}$$

is the Poissonian weighting factor of the coherent state $|\beta\rangle$ of the pump mode represented as a superposition of n-photon states. With these initial conditions the resulting state (2) can be written as

$$|\psi(t)\rangle = \sum_{n=1}^{\infty} b_n \sum_{k=0}^{n} c_{2n,k}(t) |2k, n-k\rangle \tag{14}$$

where the coefficients $c_{2n,k}(t)$ are given by (9), and they are calculated numerically.

3. Number and phase statistics

Properties of the ideal squeezed states generated in the parametric down-conversion process have been studied extensively [1–10]. It is known, for example, that for the

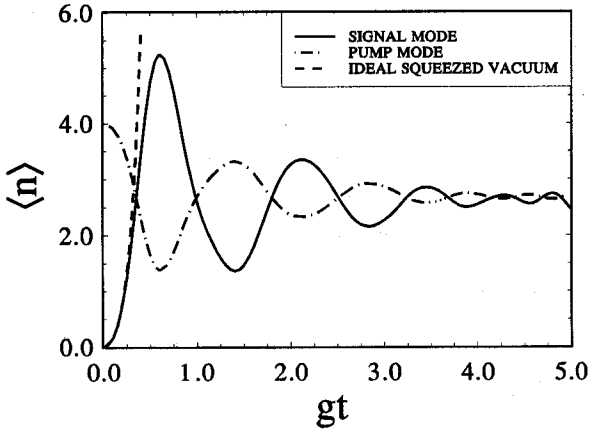

Figure 1. Evolution of the mean number of photons. The initial mean number of photons of the pump mode N_b is equal to 4 for all the figures.

squeezed vacuum the mean number of photons of the signal mode is equal to $\langle a^\dagger a\rangle = \sinh^2 r$, which is a monotonic function of the squeeze parameter r (or the evolution time gt). This means that the mean number of photons can become arbitrarily large in the long time limit (large r limit). Of course, it is a result of the parametric approximation in which the pump mode remains undepleted. If the pump mode is quantized and its dynamics included into consideration, the total energy stored in both modes is conserved, and the solutions become oscillatory. Using the state (14) of the field, we obtain for the mean number of photons of the signal mode the following expression

$$\langle a^\dagger a\rangle = \langle\psi(t)|a^\dagger a|\psi(t)\rangle$$
$$= \sum_{n=1}^{\infty} |b_n|^2 \sum_{k=0}^{n} 2k|c_{2n,k}(t)|^2 \tag{15}$$

and the mean number of photons of the pump mode can be found from the conservation relation (3)

$$\langle a^\dagger a\rangle + 2\langle b^\dagger b\rangle = 2|\beta|^2 = 2N_b. \tag{16}$$

The solutions obtained numerically from equations (15) and (16), for the mean number of photons in the pump mode $N_b = 4$, are shown in figure 1. For comparison, we have also plotted the solution for the ideal squeezed state (squeezed vacuum), which is given by $\langle a^\dagger a\rangle = \sinh^2 r$ with r related to the scaled time gt by $r = 2\sqrt{N_b}gt$. The oscillatory behaviour of the quantum solutions is clearly visible, and only at the initial stage of the evolution can the ideal squeezed state solution be treated as a good approximation to the quantum solution. One can roughly say that the first maximum of the signal intensity sets a limit to the applicability of the ideal squeezed states, i.e. there is a limit on the squeeze parameter values that can be obtained in practice. Thus, one can also expect that the states generated in the down-conversion process with a quantum pump will have different properties from those of the ideal squeezed states. To make the differences more explicit, we study in this paper the number and phase statistics of the states produced in the down-conversion process with a quantum pump and compare them to those of the ideal squeezed states.

From equation (14) we can directly derive the joint probability amplitude of finding n_a photons in the signal mode and n_b photons in the pump mode, which is given by

$$\langle n_a n_b|\psi(t)\rangle = \sum_{n=1}^{\infty} b_n \sum_{k=0}^{n} c_{2n,k}(t)\delta_{n_a,2k}\delta_{n_b,n-k}. \tag{17}$$

The joint probability $P(n_a, n_b)$ is thus given by

$$P(n_a, n_b) = |\langle n_a n_b|\psi(t)\rangle|^2 = \begin{cases} |b_{n_b+n_a/2}c_{2(n_b+n_a/2),n_a/2}(t)|^2 & \text{for } n_a \text{ even} \\ 0 & \text{for } n_a \text{ odd.} \end{cases} \tag{18}$$

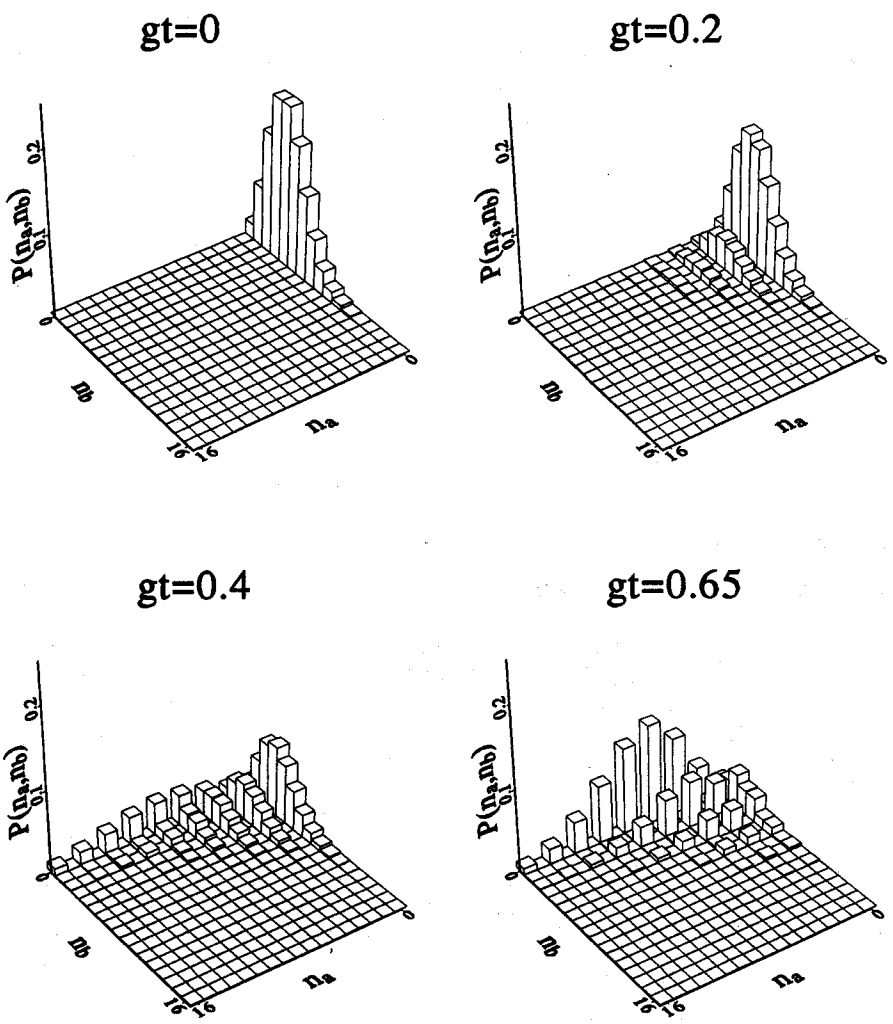

Figure 2. The joint photon number distribution $P(n_a, n_b)$, for different evolution times gt.

One immediate result of equation (18) is that only even numbers n_a can appear in the signal mode. The joint photon number distribution $P(n_a, n_b)$ depends upon the initial probabilities $|b_n|^2$ in the pump mode, and its evolution is determined by the coefficients $c_{2n,k}(t)$. In figure 2 we plot the joint distribution $P(n_a, n_b)$ against n_a and n_b, for different evolution times gt. It is seen how the initially Poissonian distribution with the mean number of photons $N_b = 4$ of the pump mode spreads over both modes during the evolution. Only even numbers n_a can appear in the signal mode, as is clearly seen in the figures. This property is the same as in the ideal squeezed states, so one can expect squeezing in the signal mode. However, for $gt = 0.65$, when the signal intensity approaches its maximum (see figure 1), one can see that almost all odd numbers n_b, except for the remnants of the initial distribution along $n_a = 0$, disappeared from the distribution. At this time of the evolution the two-photon character of the interaction is also reflected in the pump mode, so one could also expect squeezing in the pump mode. To check the squeezing properties of the field, we have plotted in figure 3 the evolution of the field quadrature variances for both the signal and pump modes. The initial phase φ_b of the pump mode is taken to be $\pi/2$ ($\beta = \sqrt{N_b}\exp(i\varphi_b)$) for this figure. As expected, squeezing appears in the out-of-phase quadrature of the signal mode at the initial stage of the evolution, and with some delay squeezing also appears in the in-phase quadrature of the pump mode. The maximum of squeezing in the pump mode is observed around $gt = 0.65$, which coincides with the maximum of the signal mode intensity. For comparison we have also plotted quadrature variance for the ideal squeezed state. In contrast to the ideal squeezed state, the squeezing in both modes disappears at later times. This corrroborates the statement that the pump quantization imposes a limit on the squeeze parameter values.

The marginal photon number distribution for the signal mode can be obtained from $P(n_a, n_b)$ by summing over n_b

$$P(n_a) = \sum_{n_b} P(n_a, n_b). \tag{19}$$

This distribution is shown in figure 4 for the time at which the signal mode exhibits the

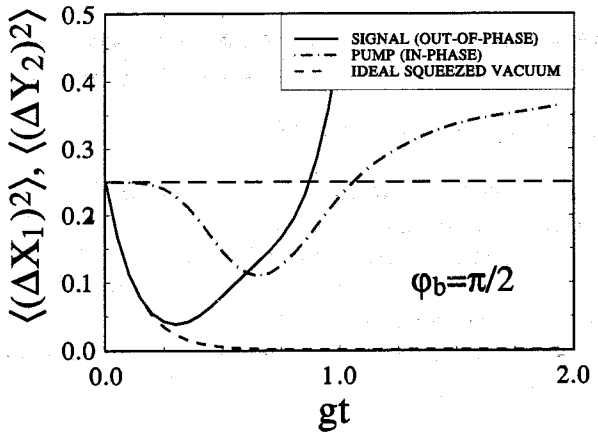

Figure 3. Evolution of the field quadrature variances $\langle(\Delta X_1)^2\rangle = \frac{1}{4}\langle[\Delta(a+a^\dagger)]^2\rangle$ and $\langle(\Delta Y_2)^2\rangle = -\frac{1}{4}\langle[\Delta(b-b^\dagger)]^2\rangle$. The horizontal line marks the level of vacuum fluctuations.

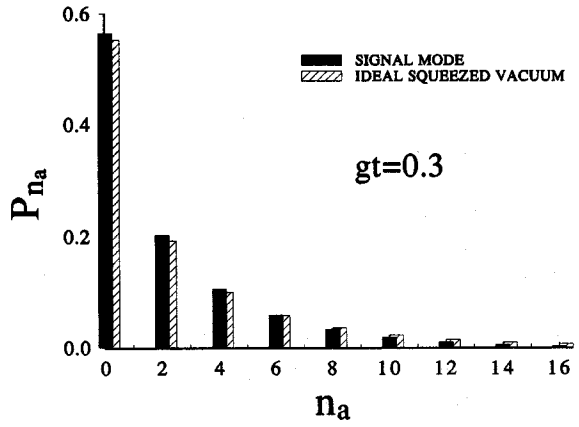

Figure 4. The photon number distribution $P(n_a)$, for $gt=0.3$, i.e. for the maximum of squeezing in the signal mode.

maximum of squeezing. For reference we also show the distribution for the ideal squeezed states assuming $r=2\sqrt{N_b}gt$. It is seen that the two distributions do not differ significantly, but the ideal squeezed vacuum exhibits a longer tail for the large n_a values.

Similarly to the mean number of photons, given by equation (15), one can calculate the variances of the number of photons for both modes. We have

$$\langle \hat{n}_a^2 \rangle = \langle (a^\dagger a)^2 \rangle$$

$$= \sum_{n=1}^{\infty} |b_n|^2 \sum_{k=1}^{n} (2k)^2 |c_{2n,k}(t)|^2 \tag{20}$$

$$\langle \hat{n}_b^2 \rangle = \langle (b^\dagger b)^2 \rangle$$

$$= \sum_{n=1}^{\infty} |b_n|^2 \sum_{k=0}^{n} (n-k)^2 |c_{2n,k}(t)|^2 \tag{21}$$

and the number of photon variances calculated in this way are plotted in figure 5. The photon number variance for the ideal squeezed vacuum is given by [27]

$$\langle (\Delta \hat{n})^2 \rangle = 2\langle \hat{n} \rangle (\langle \hat{n} \rangle + 1) = \tfrac{1}{2} \sinh^2(2r) \tag{22}$$

and is also plotted, for reference, in figure 5. The photon number fluctuations in the signal mode increase rapidly at the initial stage of the evolution, but after reaching the maximum they oscillate around a finite value (depending on the mean number of photons of the pump mode). This is in contrast to the behaviour of the photon number variance for the squeezed vacuum which grows to infinity.

Another characteristic of the field that is related to the photon number variance is the $g^{(2)}$ function defined by

$$g^{(2)} = \frac{\langle \hat{n}(\hat{n}-1) \rangle}{\langle \hat{n} \rangle^2} = 1 + \frac{\langle (\Delta \hat{n})^2 \rangle - \langle \hat{n} \rangle}{\langle \hat{n} \rangle^2} \tag{23}$$

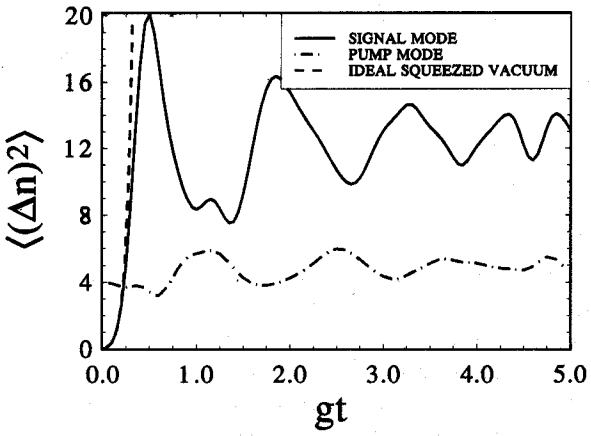

Figure 5. Evolution of the photon number variances.

which is plotted in figure 6. For the squeezed vacuum this function asymptotically approaches the value of 3. In the case of down-conversion with a quantum pump the $g^{(2)}$ function of the signal mode oscillates taking the values that dip below this asymptotic value. The photon statistics, however, are super-Poissonian for both modes. This may not seem to be true for the pump mode in view of figure 5, where it is seen that the photon number variance for the pump mode falls below 4, which is the noise level for the coherent state with mean number of photons equal to 4. However, as is evident from figure 1, the mean number of photons of the pump mode also falls below its initial value of 4, so the $g^{(2)}$ function calculated according to equation (23) at time t is greater than unity.

Since H_0 is a constant of motion, H_0^2 is also a constant of motion, and we can obtain for the fluctuations of H_0 the following relation

$$\langle(\Delta H_0)^2\rangle = \langle H_0^2\rangle - \langle H_0\rangle^2 = 4N_b(\hbar\omega)^2 \tag{24}$$

which in terms of the numbers of photons can be rewritten as

$$\langle(\Delta\hat{n}_a)^2\rangle + 4\langle(\Delta\hat{n}_b)^2\rangle + 4\langle\Delta\hat{n}_a\Delta\hat{n}_b\rangle = 4N_b. \tag{25}$$

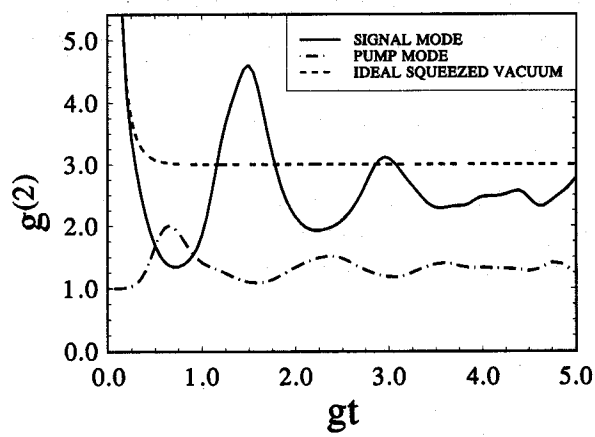

Figure 6. Evolution of the $g^{(2)}$ function.

Formula (25) establishes the relation between the fluctuations of the individual-mode photon numbers and the intermode photon number correlation. All these quantities on the left-hand side of (25) can be calculated numerically using the state (14), so that formula (25) can serve as a test of numerical precision. The value of $4N_b$ sets the level of fluctuations for the initially coherent state of the pump mode.

The quantity conjugated to the photon number is the field phase. Recently, Pegg and Barnett [22–24] have introduced the Hermitian phase formalism, which allows construction of the Hermitian phase operator for the field mode and, as a result, systematic study of the phase properties of the field. We use here the Pegg–Barnett phase formalism to study the phase properties of the field produced in the down-conversion process with a quantum pump. This formalism is based on introducing a finite $(s+1)$-dimensional space Ψ spanned by the number states $|0\rangle, |1\rangle, \ldots, |s\rangle$, for a given mode of the field. The Hermitian phase operator operates on this finite space and, after all necessary expectation values have been calculated in Ψ, the value of s is allowed to tend to infinity. A complete orthonormal basis of $(s+1)$ states is defined on Ψ as

$$|\theta_m\rangle \equiv \frac{1}{\sqrt{s+1}} \sum_{n=1}^{s} \exp(\mathrm{i}n\theta_m)|n\rangle \tag{26}$$

where

$$\theta_m \equiv \theta_0 + \frac{2\pi m}{s+1} \qquad (m=0,1,\ldots,s). \tag{27}$$

The value of θ_0 is arbitrary and defines a particular basis set of $(s+1)$ mutually orthogonal phase states. The Hermitian phase operator is defined as

$$\hat{\phi}_\theta \equiv \sum_{m=0}^{s} \theta_m |\theta_m\rangle\langle\theta_m| \tag{28}$$

where the subscript θ indicates the dependence on the choice of θ_0. The phase states (26) are eigenstates of the phase operator (28) with the eigenvalues θ_m restricted to lie within a phase window between θ_0 and $\theta_0 + 2\pi$. The unitary phase operator $\exp(\mathrm{i}\hat{\phi}_\theta)$ is defined as the exponential function of the Hermitian operator $\hat{\phi}_\theta$. This operator acting on the eigenstate $|\theta_m\rangle$ gives the eigenvalue $\exp(\mathrm{i}\theta_m)$, and it has the form [23, 24]

$$\exp(\mathrm{i}\hat{\phi}_\theta) \equiv \sum_{n=0}^{s-1} |n\rangle\langle n+1| + \exp[\mathrm{i}(s+1)\theta_0]|s\rangle\langle 0|. \tag{29}$$

The last term in (29) ensures the unitarity of this operator. The first sum reproduces the Susskind–Glogower [28, 29] phase operator in the limit $s \to \infty$.

The expectation value of the phase operator (28) in a state $|\psi\rangle$ is given by

$$\langle\psi|\hat{\phi}_\theta|\psi\rangle = \sum_{m=0}^{s} \theta_m |\langle\theta_m|\psi\rangle|^2 \tag{30}$$

where $|\langle\theta_m|\psi\rangle|^2$ gives the probability of being found in the phase state $|\theta_m\rangle$. The density of phase states is $(s+1)/2\pi$, so in the continuum limit, as s tends to infinity, we can

write equation (30) as

$$\langle\psi|\hat{\phi}_\theta|\psi\rangle=\int_{\theta_0}^{\theta_0+2\pi}\theta P(\theta)\,\mathrm{d}\theta \tag{31}$$

where the continuum phase distribution $P(\theta)$ is introduced by

$$P(\theta)=\lim_{s\to\infty}\frac{s+1}{2\pi}|\langle\theta_m|\psi\rangle|^2 \tag{32}$$

where θ_m has been replaced by the continuous phase variable θ. Once the phase distribution function $P(\theta)$ is known, all the quantum mechanical phase expectation values can be calculated with this function in a classical manner by integrating over θ. The choice of θ_0 defines a particular window of phase values.

In our case of a field produced in the down-conversion process with a quantum pump, the state of the field (14) is in fact a two-mode state, and the phase formalism must be generalized to the two-mode case. The generalization is straightforward and obvious, and for the state (14) we get

$$\begin{aligned}|\langle\theta_{m_a}|\langle\theta_{m_b}|\psi(t)\rangle=(s_a+1)^{-1/2}\\ \times\sum_{n=0}^{s_a}b_n\sum_{k=0}^{n}\exp\{-\mathrm{i}[2k\theta_{m_a}+(n-k)\theta_{m_b}]\}c_{2n,k}(t).\end{aligned} \tag{33}$$

We use the indices a and b to distinguish between the signal (a) and pump (b) modes. There is still a freedom of choice in (33) of the values of $\theta_0^{a,b}$, which define the phase values window. We can choose these values at will, so we take them as

$$\theta_0^{a,b}=\varphi_{a,b}-\pi s_{a,b}/(s_{a,b}+1) \tag{34}$$

and we introduce the new phase values

$$\theta_{\mu_{a,b}}=\theta_{m_{a,b}}-\varphi_{a,b} \tag{35}$$

where the new phase labels $\mu_{a,b}$ run in unit steps between the values $-s_{a,b}/2$ and $s_{a,b}/2$. This means that we symmetrize the phase windows for the signal and pump modes with respect to the phases φ_a and φ_b, respectively.

On inserting (34) and (35) into (33), taking the modulus squared of (33), and taking the continuum limit by making the replacement

$$\sum_{\mu_{a,b}=-s_{a,b}/2}^{s_{a,b}/2}\frac{2\pi}{s_{a,b}+1}\to\int_{-\pi}^{\pi}\mathrm{d}\theta_{a,b} \tag{36}$$

we arrive at the continuous joint probability distribution for the continuous variables θ_a and θ_b, which has the form

$$\begin{aligned}P(\theta_a,\theta_b)=\frac{1}{(2\pi)^2}\Bigg|\sum_{n=0}^{\infty}|b_n|\exp(-\mathrm{i}n\varphi_b)\sum_{k=0}^{n}C_{2n,k}(t)\\ \times\exp\{-\mathrm{i}[2k\theta_a+(n-k)\theta_b+k(2\varphi_a-\varphi_b)]\}\Bigg|^2.\end{aligned} \tag{37}$$

The distribution (37) is normalized so that

$$\int_{-\pi}^{\pi}\int_{-\pi}^{\pi}P(\theta_a,\theta_b)\,\mathrm{d}\theta_a\,\mathrm{d}\theta_b=1. \tag{38}$$

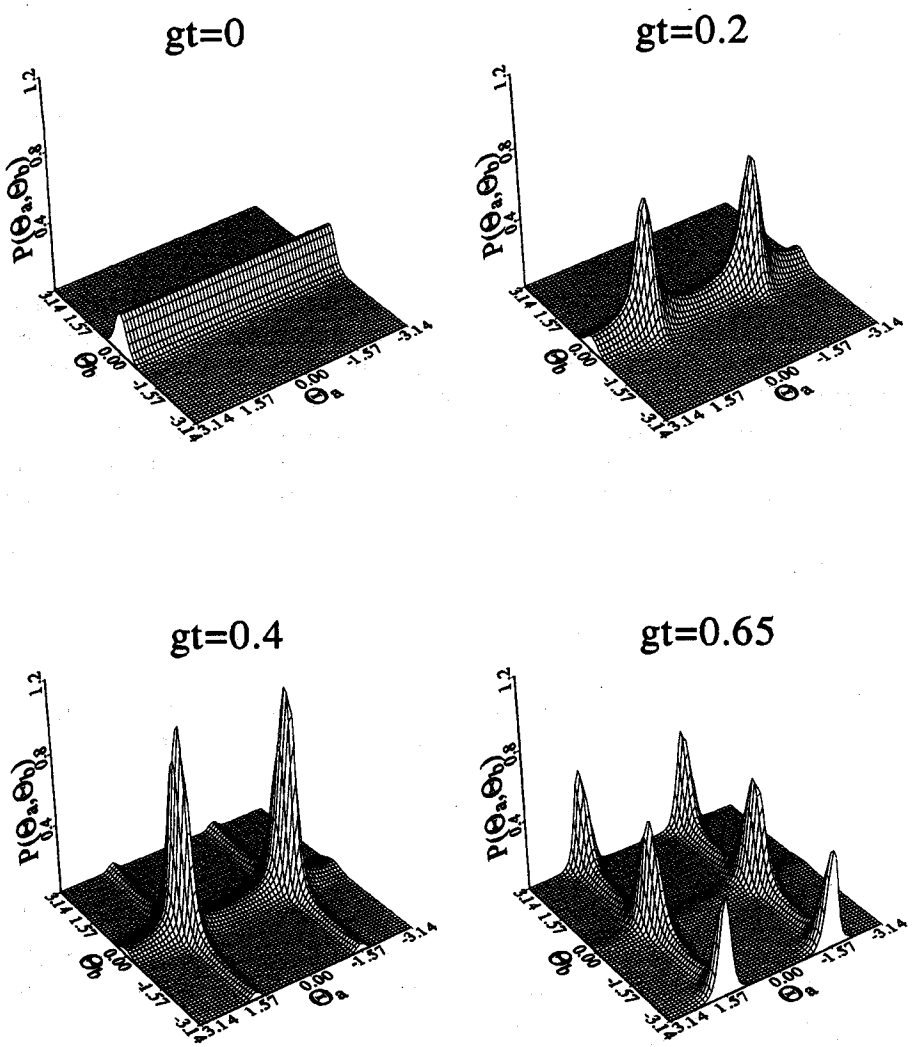

Figure 7. The joint phase distribution $P(\theta_a, \theta_b)$, for different evolution times gt.

To fix the phase windows for θ_a and θ_b, we have to assign to φ_a and φ_b particular values. It is interesting to note that the distribution $P(\theta_a, \theta_b)$ given by (37) depends on the phase difference $2\varphi_a - \varphi_b$ only. This reproduces the classical phase relation for the parametric amplifier, and classically this quantity should be equal to $-\pi/2$ to get the amplification of the signal mode (if the coupling constant g is positive). Such choice means that a peak should appear in the phase distribution at $\theta_a = 0$. As will become clear later, the phase distribution for the two-photon down-conversion process exhibits a two-peak structure along the θ_a direction, and the choice of the window with a peak for $\theta_a = 0$ would maximize the phase variance. To minimize the phase variance we choose $2\varphi_a - \varphi_b = \pi/2$. The phase distribution $P(\theta_a, \theta_b)$ is illustrated in figure 7, for the mean number of photons N_b in the pump mode equal to 4 and different evolution times gt. This distribution can be compared with the photon number distribution presented in figure 2. The two-photon character of the process, which is seen in the photon number distribution by the presence of holes in the distribution of odd n_a, is

reflected in the phase distribution by the presence of two peaks along the θ_a direction. It is interesting to see that for $gt = 0.65$, i.e. for the value of the maximum intensity of the signal mode and the maximum value of squeezing in the pump mode (compare figures 1 and 3), the phase distribution along the θ_b direction of pump mode assumes the two-peak structure characteristic of the squeezed states. This means that the state of the pump mode becomes close to the squeezed state. The photon number distribution (figure 2) with holes that appeared for odd n_b confirms this statement. So, the squeezing has been transferred from the signal mode to the pump mode. A bifurcation of the phase distribution along the θ_b direction indicates the transition of the process from the down-conversion regime to the second-harmonic generation regime. In the long time limit the phase distribution goes through a sequence of such bifurcations towards the multipeak structure, which means randomization of phases [20].

Integrating $P(\theta_a, \theta_b)$ over one of the phases leads to the marginal phase distributions $P(\theta_a)$ and $P(\theta_b)$ for the phases θ_a and θ_b of the individual modes. We have

$$P(\theta_a) = \int_{-\pi}^{\pi} P(\theta_a, \theta_b)\, \mathrm{d}\theta_b$$

$$= \frac{1}{2\pi}\left\{1 + 2\,\mathrm{Re}\sum_{n>n'} |b_n||b_{n'}| \sum_{k=0}^{n}\sum_{k'=0}^{n'} c_{2n,k}(t)c^*_{2n',k'}(t) \right.$$

$$\left. \times \exp[-\mathrm{i}(k-k')(2\theta_a + 2\varphi_a - \varphi_b)]\delta_{n-n',k-k'}\right\} \tag{39}$$

and

$$P(\theta_b) = \frac{1}{2\pi}\left\{1 + 2\,\mathrm{Re}\sum_{n>n'} |b_n||b_{n'}| \sum_{k=0}^{n'} c_{2n,k}(t)c^*_{2n',k}(t)\exp[-\mathrm{i}(n-n')\theta_b]\right\}. \tag{40}$$

The phase distribution $P(\theta_a)$ for the signal mode is shown in figure 8 for $gt = 0.3$, i.e. for the time at which the squeezing in the signal mode has its maximum value. For comparison we show the phase distribution for the ideal squeezed vacuum for

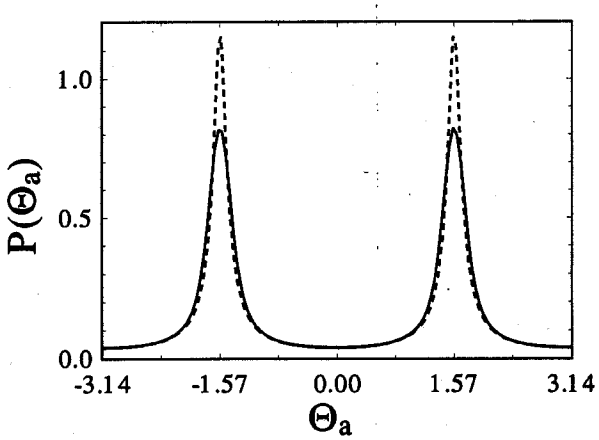

Figure 8. The phase distribution $P(\theta_a)$, for $gt = 0.3$.

$r=2\sqrt{N_b}gt=1.2$. The phase distribution for the squeezed vacuum can be obtained from the known number state decomposition of the squeezed vacuum state [27]

$$|0\rangle_{(r,\eta)}=\sum_{n=0}^{\infty} a_n|n\rangle \tag{41}$$

where

$$a_n=\begin{cases}\dfrac{(-1)^{n/2}}{\sqrt{\cosh r}}\dfrac{\sqrt{n!}}{(n/2)!}(\tfrac{1}{2}\tan r)^{n/2}\exp(\mathrm{i}n\eta) & n \text{ even}\\ 0 & n \text{ odd}\end{cases} \tag{42}$$

with r being the squeeze parameter and η being the phase that we assume equal to zero later on. With the amplitudes (42) the phase distribution can be calculated according to the formula

$$\begin{aligned}P(\theta)&=\frac{1}{2\pi}\left|\sum_{n=0}^{\infty} a_n\,\mathrm{e}^{-\mathrm{i}n\theta}\right|^2\\ &=\frac{1}{2\pi}\left(1+2\sum_{n>m} a_n a_m\cos[(n-m)\theta]\right)\end{aligned} \tag{43}$$

where we have assumed a_n real. Since only the amplitudes with even n are different from zero, the phase distribution is periodic in θ with the period π, i.e. within the phase window $-\pi\le\theta\le\pi$ there are two identical, symmetrically disposed phase peaks. As seen from figure 8, the phase distribution for the squeezed vacuum is narrower than the distribution in the case with a quantum pump. Comparing figures 4 and 8, we see that the squeezed vacuum has a broader photon number distribution and narrower phase distribution than the signal mode in the down-conversion with a quantum pump.

The Pegg–Barnett phase formalism allows the phase variances to be calculated for the individual-mode phases as well as the intermode phase correlation function. The phase variance for the signal mode can be calculated according to the formula

$$\begin{aligned}\langle(\Delta\hat{\phi}_{\theta_a})^2\rangle&=\langle\hat{\phi}_{\theta_a}\rangle^2\\ &=\int_{-\pi}^{\pi}\theta_a^2 P(\theta_a)\,\mathrm{d}\theta_a\\ &=\tfrac{1}{3}\pi^2+\mathrm{Re}\sum_{n>n'}|b_n||b_{n'}|\frac{\exp[-\mathrm{i}(n-n')(2\varphi_a-\varphi_b)]}{(n-n')^2}\\ &\quad\times\sum_{k=n-n'}^{n} c_{2n,k}(t)c^*_{2n',k-(n-n')}(t)\end{aligned} \tag{44}$$

and for the pump mode we have

$$\begin{aligned}\langle(\Delta\hat{\phi}_{\theta_b})^2\rangle&=\int_{-\pi}^{\pi}\theta_b^2 P(\theta_b)\,\mathrm{d}\theta_b\\ &=\tfrac{1}{3}\pi^2+4\mathrm{Re}\sum_{n=>n'}|b_n||b_{n'}|\frac{(-1)^{n-n'}}{(n-n')^2}\sum_{k=0}^{n'} c_{2n,k}(t)c^*_{2n',k}(t)\end{aligned} \tag{45}$$

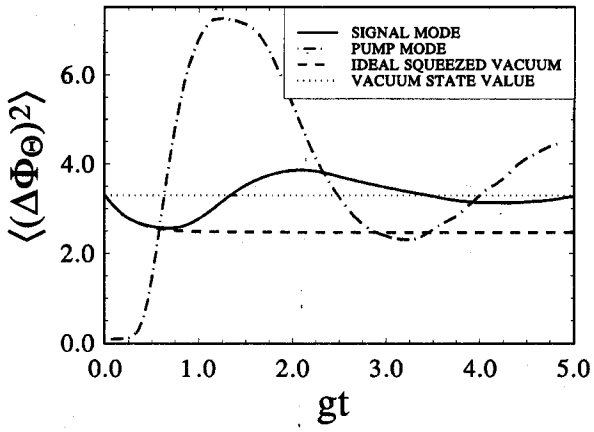

Figure 9. Evolution of the phase variances.

where we have used (39) and (40), and we take $2\varphi_a - \varphi_b = \pi/2$. The phase variances are plotted in figure 9, and for reference we plot the phase variance for the squeezed vacuum. The squeezed vacuum phase variance asymptotically approaches the value $\pi^2/4$, which corresponds to the phase distribution with two symmetrically placed delta functions

$$P(\theta) = \tfrac{1}{2}[\delta(\theta - \tfrac{1}{2}\pi) + \delta(\theta + \tfrac{1}{2}\pi)]. \tag{46}$$

The phase fluctuations in the signal mode have oscillatory character, although at the initial stage of the evolution they are indistinguishable from those of the squeezed vacuum, and at the long time limit they approach the value $\pi^2/3$ characteristic of the uniformly distributed phase [23, 24]. The phase fluctuations in the pump mode start from the small value characteristic for the initial coherent state and grow rapidly, next, they oscillate approaching the value $\frac{1}{3}\pi^2$. So, the quantum fluctuations lead to randomization of the phases for both modes in the long-time limit.

Since the number and phase are two conjugate quantities, they obey the uncertainty relation [24]

$$\Delta n \Delta\phi_\theta \geq \tfrac{1}{2}|\langle[\hat{n}, \hat{\phi}_\theta]\rangle|. \tag{47}$$

Knowing the variances for the numbers of photons and phases for both modes we can calculate the uncertainty products

$$\Delta n_{a,b} \Delta\phi_{\theta_{a,b}} = [\langle(\Delta\hat{n}_{a,b})^2\rangle\langle(\Delta\hat{\phi}_{\theta_{a,b}})^2\rangle]^{1/2}. \tag{48}$$

The number–phase commutator can also be easily evaluated for any physical state $|p\rangle$ from the relation [24]

$$\langle p|[\hat{\phi}_\theta, \hat{n}]|p\rangle = -\mathrm{i}[1 - 2\pi P(\theta_0)]. \tag{49}$$

In figure 10 we have plotted both the uncertainty product and one-half of the modulus of the expectation value of the phase–number commutator (evaluated according to (49) with $\theta_0 = -\pi$). It is seen that the uncertainty product remains finite in the long-time limit for a finite mean number of initial photons, which is in contrast to the squeezed vacuum for which it tends to infinity. For any finite r the ideal squeezed vacuum, however, can be considered as a physical state and we can apply (49) to calculate the mean value of the number-phase commutator. When r tends to infinity,

the phase distribution tends to the form of two delta functions given by (46), i.e. $P(-\pi)$ tends to zero, and asymptotically the expectation value of the commutator tends to $-\mathrm{i}$. This is clearly seen from figure 10, where the asymptotic value of $\frac{1}{2}$ is reached for the ideal squeezed vacuum. So, this is the infinitely growing photon number uncertainty that causes the infinite growth of the number–phase uncertainty product for the ideal squeezed vacuum.

The notion of number and phase squeezing can be introduced for the two conjugate quantities, and the degree of number and phase squeezing can be defined by [30, 31]

$$S_n = \frac{\langle(\Delta\hat{n})^2\rangle - \frac{1}{2}|\langle[\hat{n}, \hat{\phi}_\theta]\rangle|}{\frac{1}{2}|\langle[\hat{n}, \hat{\phi}_\theta]\rangle|} \tag{50}$$

$$S_\phi = \frac{\langle(\Delta\hat{\phi}_\theta)^2\rangle - \frac{1}{2}|\langle[\hat{n}, \hat{\phi}_\theta]\rangle|}{\frac{1}{2}|\langle[\hat{n}, \hat{\phi}_\theta]\rangle|}. \tag{51}$$

These two quantities give the relative quantum fluctuations, with respect to the minimum uncertainty, and the value of -1 means perfect squeezing of the photon number (or the phase). We have plotted the two squeezing parameters for the signal mode in figure 11 for the pump mode in figure 12. There is initially number squeezing in the signal mode and phase squeezing in the pump mode.

The number squeezing, which can also be considered as amplitude squeezing, in the signal mode is understandable because this mode starts from the vacuum, that is, the eigenstate of the photon number operator. We should, however, emphasize that the number squeezing, defined by (50), does not imply sub-Poissonian photon statistics, i.e. $g^{(2)}<1$. The two are different characteristics of the photon number noise, and we can see here that the signal mode exhibits number squeezing and at the same time is super-Poissonian.

The phase squeezing, as defined by (51), gives us information about the degree of squeezing in $\hat{\phi}_\theta$. For the coherent state with $|\alpha|>1$ the phase is squeezed, and for high

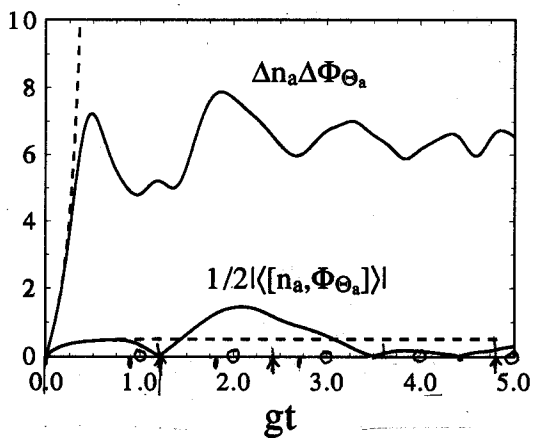

Figure 10. Evolution of the number–phase uncertainties for the signal mode.

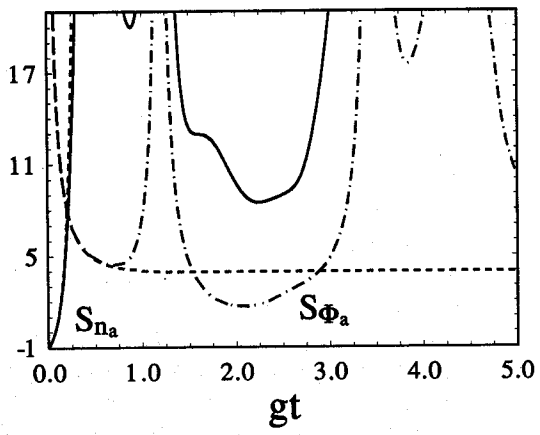

Figure 11. Evolution of the number and phase squeezing parameters, defined by equations (50) and (51), for the signal mode.

intensities of coherent fields S_ϕ tends to -1, which means that such states are close to the phase states with well defined phase. In our case, we observe phase squeezing in the initially coherent pump mode which is, however, revoked rapidly during the evolution.

It is interesting to see the sharp peaks of relative phase fluctuations that appear in both modes. They are related to the minima of intensities in particular modes (see figure 1) and the minima of the commutator expectation values (see figure 10). There is no such peak for the ideal squeezed vacuum. Moreover, from the asymptotic value $\frac{1}{4}\pi^2$ of the phase variance and the asymptotic behaviour of the number-phase commutator expectation value, we get the asymptotic value of $\frac{1}{2}\pi^2 - 1$ for the phase squeezing of the ideal squeezed vacuum. Thus the phase properties of the signal mode are essentially different from those of the ideal squeezed vacuum in the oscillatory

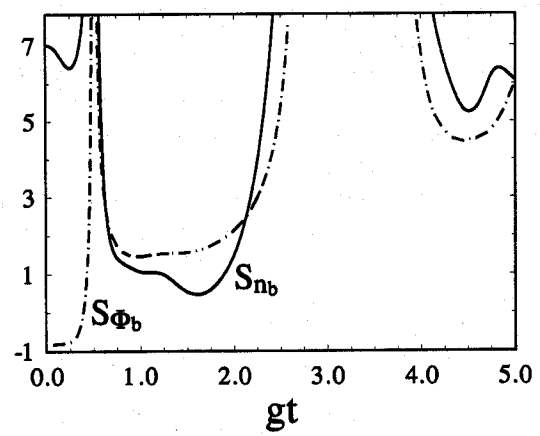

Figure 12. Same as in figure 11, but for the pump mode.

part of the evolution, but they are similar in the initial part of the evolution before the first maximum of the signal intensity has been reached.

4. Conclusions

We have studied the photon number and phase quantum fluctuations in the field generated in the down-conversion process with a quantum pump. That is, we have used a fully quantum description of both modes of the field avoiding the parametric approximation. The method of numerical diagonalization of the interaction Hamiltonian has been employed to find the quantum evolution of the system. This method allowed us to calculate and illustrate graphically the evolution of a number of quantities characterizing the number and phase quantum fluctuations of the field. To deal with the phase quantum fluctuations we have applied the Hermitian phase formalism of Pegg and Barnett, which allows the quantum phase of the field to be treated on an equal footing with the photon number. We have studied and compared quantum fluctuations in both conjugate quantities for the signal and pump modes. The properties of the signal mode generated in the down-conversion process with a quantum pump have been compared to those of the ideal squeezed vacuum resulting in the parametric approximation.

Our results show that the quantum character of the pump mode, when taken into account, essentially changes the properties of the field at later stages of evolution, while at earlier stages of evolution the signal mode properties are very close to those of the ideal squeezed vacuum. The quantum fluctuations of the pump mode set, in fact, a limit on the values of the squeeze parameters that can be obtained in a real physical situation.

It is also seen from our results that the two-photon character of the process is clearly reflected in the photon number distribution of the signal mode through the absence of odd numbers of photons (or more precisely through the presence of pairs of photons only), and in the phase distribution it is reflected through the two-peak structure of the signal-mode phase distribution. Moreover, it is seen that the pump mode can also become squeezed, and at the time of maximum squeezing the photon number distribution and the phase distribution of the pump mode exhibit the same characteristic features, although not in their pure form. This can be considered as an illustration of the conjugate character of the number and phase variables.

We have also studied the number–phase uncertainty product as well as the expectation value of their commutator. Contrary to the ideal squeezed vacuum, the uncertainty product remains finite (for finite initial mean number of photons N_b) in the long time limit. Since the expectation value of the number–phase commutator sets the lower bound for the uncertainty product, it is sometimes convenient to characterize the number and phase quantum fluctuations as relative quantities calculated with respect to the minimum uncertainty. This leads to the notion of number and phase squeezing. The degree of such squeezing for both modes has also been calculated showing the presence of sharp peaks of the phase squeezing.

In our numerical calculations we have assumed the mean number of initial photons in the pump mode (being in a coherent state) as $N_b = 4$. This value is small enough to make the numerical calculations fast and reliable but, nevertheless, allows some classical features of the field to be observed (appearing for $N_b \gg 1$) while the quantum properties of the field are still clearly visible.

References

[1] Takahasi H 1965 *Adv. Commun. Syst.* **1** 227
[2] Stoler D 1970 *Phys. Rev.* D **1** 3217; 1971 *Phys. Rev.* D **4** 1925
[3] Lu E Y C 1971 *Nuovo Cimento Lett.* **2** 1241
[4] Yuen H P 1976 *Phys. Rev.* A **13** 2226
[5] Hollenhorst J N 1979 *Phys. Rev.* D **19** 1669
[6] Caves C M 1981 *Phys. Rev.* D **23** 1693
[7] Friberg S, Hong C K and Mandel L 1985 *Phys. Rev. Lett.* **54** 2011
[8] Reid M D and Walls D F 1986 *Phys. Rev.* A **34** 1260
[9] Ou Z Y and Mandel L 1988 *Phys. Rev. Lett.* **61** 50
[10] Tan S M and Walls D F 1989 *Opt. Commun.* **71** 235
[11] Wu L A, Kimble H J, Hall J L and Wu H 1986 *Phys. Rev. Lett.* **57** 2520
[12] Heidmann A, Horowicz R, Reynaud S, Giacobino E, Fabre C and Camy G 1987 *Phys. Rev. Lett.* **59** 2555
[13] Slusher R, Grangier P, LaPorta A, Yurke B and Potasek M 1987 *Phys. Rev. Lett.* **59** 2566
[14] Pereira S, Xiao M, Kimble H J and Hall J 1988 *Phys. Rev.* A **38** 4931
[15] Tapster P R, Rarity J G and Satchell J S 1988 *Phys. Rev.* A **37** 2963
[16] Debuischert T, Reynaud S, Heidmann A, Giacobino E and Fabre C 1989 *Quantum Opt.* **1** 3
[17] Vaccaro J A and Pegg D T 1989 *Opt. Commun.* **70** 529
[18] Schleich W, Horowicz R J and Varro S 1989 *Phys. Rev.* A **40** 7405
[19] Grønbech-Jensen N, Christiansen P L and Ramanujam P S 1989 *J. Opt. Soc. Am.* B **6** 2423
[20] Gantsog Ts, Tanaś R and Zawodny R 1991 *Opt. Commun.* **82** 345
[21] Walls D F and Barakat R 1970 *Phys. Rev.* A **1** 446
[22] Pegg D T and Barnett S M 1988 *Europhys. Lett.* **6** 483
[23] Barnett S M and Pegg D T 1989 *J. Mod. Opt.* **36** 7
[24] Pegg D T and Barnett S M 1989 *Phys. Rev.* A **39** 1665
[25] Gantsog Ts, Tanaś R and Zawodny R 1991 *Phys. Lett.* **155**A 1
[26] Tanaś R, Gantsog Ts and Zawodny R 1991 *Quantum Opt.* **3** 221
[27] London R and Knight P L 1987 *J. Mod. Opt.* **34** 709
[28] Susskind L and Glogower J 1964 *Physics* **1** 49
[29] Carruthers P and Nieto M M 1968 *Rev. Mod. Phys.* **40** 411
[30] Wódkiewicz K and Eberly J H 1985 *J. Opt. Soc. Am.* B **2** 458
[31] Bužek V, Wilson-Gordonj A D, Knight P L and Lai W K 1991 *Phys. Rev.* A in press